Journal of Luminescence 242 (2022) 118558

Contents lists available at ScienceDirect

Journal of Luminescence

journal homepage: www.elsevier.com/locate/jlumin

Design of Experiments (DoE) method for solar protective films via UV–Vis and NIR spectrophotometry measurements

Eriberto Oliveira do Nascimento [a], Matheus José Pires Becatti [a], Linda V.E. Caldas [b], Lucas Nonato de Oliveira [a,b,*]

[a] Instituto Federal de Educação, Ciência e Tecnologia de Goiás-IFG, Campus Goiânia, Rua 75, no 46, 74055-110, Goiânia, GO, Brazil
[b] Instituto de Pesquisas Energéticas e Nucleares, Comissão Nacional de Energia Nuclear-IPEN/CNEN, Av. Prof. Lineu Prestes, 2242, 05508-000, São Paulo, SP, Brazil

A R T I C L E I N F O

Keywords:
Design of experiments
Multiple linear regression
Solar protective films

A B S T R A C T

Individual dosimetry and the shielding of sun rays are needed for people in homes, at workplaces and vehicles when exposed to Ultraviolet Radiation (UVR) and/or Infrared Radiation (IR). Usually, the efficacy of Solar Protective Films (SPF) has been recognized as an important public health concern. So, this work aimed to verify, using the Design of Experiments (DoE) and Multiple Linear Regression (MLR) methods, the evaluation of solar films using the UV–Vis and NIR (Near Infrared) spectrophotometry technique for absorbance readings. In addition, the significance of the SPF manufacturing origin and glass color were evaluated. Four types of SPF, named G05, G20, G35 and WB, were tested and layered within dark and light glasses. The absorbance readings were used in a 2^k factorial design analysis, then the one-way ANOVA Test and the Bonferroni Test were used to assess the statistical significance of each factor. The results showed that the statistical error, using the Root Mean Square Percentage Error (RMSPE) and the Mean Absolute Percentage Error (MAPE) methods, showed values less than 0.014% between the measured and the predicted ones, indicating excellent accuracy. In conclusion, DoE and MLR methods are suitable to be used in the investigation of the association between SPF and glass materials.

1. Introduction

Numerous researchers have demonstrated the harmful effects that Ultraviolet Radiation (UVR) can cause in biological tissues, highlighting that the most critical regions are comprised in the range of UVA: 400-315 nm; UVB: 315-280 nm; and UVC: 280-100 nm [1]. In these studies, a variety of consequences due to UVA exposure were emphasized, such as early aging (photoaging), skin cancer, aesthetic damage, sunburn and a plethora of physical and chemical reactions that can lead to temporary or permanent biological damage [2,3], i.e., vision loss due to direct sun exposure [4].

Several glass types can be used in vehicles and homes as a protection solution, aiming to reduce the overall exposure to UVR. Some of these glasses include tempered, annealed, soda lime, reflective, low emissivity, laminate, and insulating types [5]. Each of them has specific characteristics about the way that it generates the protection factor, e.g., depending upon the user purpose, which can be the regulation of visible light to a chosen environment or the total blocking effect. Ergonomically speaking, glasses coupled in helmets of welding workers must provide a critical level of safety to their users regarding lighting blocking and lowering the overall ergonomic risk [6,7].

Moreover, studies on automotive glass demonstrated the need for research on radiation incidence control, being the development of new materials the most important area. As a result, the development of these new materials, they can help individuals not to be exposed to elevate levels of UVR during their lifetime, then preventing some of the previously mentioned health problems [8–10].

The UV absorbances from the solar protective films associated with glass were evaluated using the 2^k factorial design, which used as controllable factors the glass color and the solar protective films from four distinct manufacturers. Seeking to get a global picture over the various solar protective films evaluated, it was necessary to use all combinations. To this purpose, the 2^k factorial design is useful, since it is a methodology that can provide predictive information about the experiment [11,12]. Consequently, this model can be associated with the Multiple Linear Regression method which also provides analytical information through a semi-empirical model.

The aim of this work was to investigate for the first time, the use of

* Corresponding author. Instituto Federal de Educação, Ciência e Tecnologia de Goiás-IFG, Rua 75, no 46, 74055-110, Goiânia, GO, Brazil.
E-mail address: lucas@ifg.edu.br (L. Nonato de Oliveira).

https://doi.org/10.1016/j.jlumin.2021.118558
Received 8 January 2021; Received in revised form 22 October 2021; Accepted 25 October 2021
Available online 30 October 2021

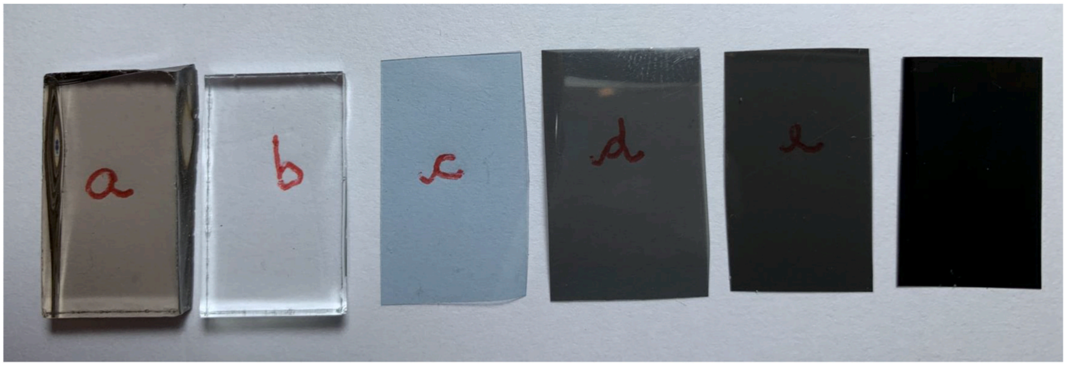

Fig. 1. Samples used in this work from left to right are: dark glass, light glass, WB, G35, G20 and G05. The samples G35, G20 and G05 were manufactured by Window premium® and the sample WB by Window blue®. Both types of glasses are commercial soda-lime.

Table 1
Factor definition for 2^k factorial designs. The natural factors are solar protection films and glass, coded as factors A and B, respectively.

	Natural Factor	
	Solar protection film	Glass
Natural level	Type 1	Light
	Type 2	Dark
Coded Factor		
	A	B
Coded level	−1	−1
	+1	+1

Table 2
General Contrast Matrix for 2^k factorial design. The run means the possible combinations for factors A, B and AB. The absorbance response y is related to the effects measured in the UV–Vis spectrophotometer.

Run	x_1 *(A)*	x_2 *(B)*	x_3 *(AB)*	y_i
1	−1	−1	+1	y_1
2	+1	−1	−1	y_2
3	−1	+1	−1	y_3
4	+1	+1	+1	y_4

Table 3
All possible combinations between solar protection films and glasses can be observed. The determination of factors −1 for the glass was for the lower absorbance values and +1 for the higher absorbance values. For the films, the values followed the same consensus, −1 for lower absorbance values and +1 for the higher absorbance values.

P1 = G20/G05
G20 – G05 [-1 +1] and Light glass – Dark glass [−1 +1]

Run	X1	X2	X1X2
1	G20	Light glass	G20/ Light_glass
2	G05	Light glass	G05/ Light_glass
3	G20	Dark glass	G20/ Dark_glass
4	G05	Dark glass	G05/ Dark_glass

P2 = G35/G05
G35 – G05 [-1 +1] and Light glass – Dark glass [−1 +1]

Run	X1	X2	X1X2
1	G35	Light glass	G35/ Light_glass
2	G05	Light glass	G05/ Light_glass
3	G35	Dark glass	G35/ Dark_glass
4	G05	Dark glass	G05/ Dark_glass

P3 = WB/G05
WB – G05 [-1 +1] and Light glass – Dark glass [−1 +1]

Run	X1	X2	X1X2
1	WB	Light glass	WB/ Light_glass
2	G05	Light glass	G05/ Light_glass
3	WB	Dark glass	WB/ Dark_glass
4	G05	Dark glass	G05/ Dark_glass

P4 = G35/G20
G35 – G20 [-1 +1] and Light glass – Dark glass [−1 +1]

Run	X1	X2	X1X2
1	G35	Light glass	G35/ Light_glass
2	G20	Light glass	G20/ Light_glass
3	G35	Dark glass	G35/ Dark_glass
4	G20	Dark glass	G20/ Dark_glass

P5 = G20/WB
G20 – WB [-1 +1] and Light glass – Dark glass [−1 +1]

Run	X1	X2	X1X2
1	WB	Light glass	WB/ Light_glass
2	G20	Light glass	G20/ Light_glass
3	WB	Dark glass	WB/ Dark_glass
4	G20	Dark glass	G20/ Dark_glass

P6 = G35/WB
G35 – WB [-1 +1] and Light glass – Dark glass [−1 +1]

Run	X1	X2	X1X2
1	G35	Light glass	G35/ Light_glass
2	WB	Light glass	WB/ Light_glass
3	G35	Dark glass	G35/ Dark_glass
4	WB	Dark glass	WB/ Dark_glass

the Design of Experiments (DoE) and Multiple Linear Regression (MLR) methods in measurements with solar protection film in association with light and dark glasses, using as an evaluation technique the UV–Vis and NIR spectrophotometry.

2. Physics and chemistry context

The UV–Vis and NIR spectroscopy technique was used since it is a low-cost solution and a non-destructive test widely available [13–15]. It is well known that the proper design of lighting exposure in indoor environments reverberates in a multidimensional field, which covers a vast range of aspects, passing through the industry [16] and reaching the educational system as well [17]. So, the interaction of human activities with an environment must occur by means of adequate lighting conditions, as consolidated in the current literature [18].

In the physics context, there is one aspect that is customarily underrepresented in the ergonomics community, which is the influence of UV-radiation exposure and its relations to worker safety [19]. A common misconception arises when one may think, erroneously, that a dark glass or any solar protection film can reduce UV-radiation, but this is not always true. For example, the common silicate glass indeed allows the transmission of the UVR [16]. In other words, glasses may present higher transmittance and lower absorbance at a specific wavelength, or may even manifest a nonlinear behavior depending upon the glass is doped or not [20]. This phenomenon can be modeled by Lambert-Beer Law [21], as shown in Eq. (1); it predicts the quantity of absorbed (A = absorbance) or transmitted (T = transmittance) light in the medium (association with film and glass). The values were obtained, using:

$$A = \log_{10}\left(\frac{I_0}{I}\right) = -\log_{10} T \tag{1}$$

where I_0 and I are the incident and transmitted light intensities. The

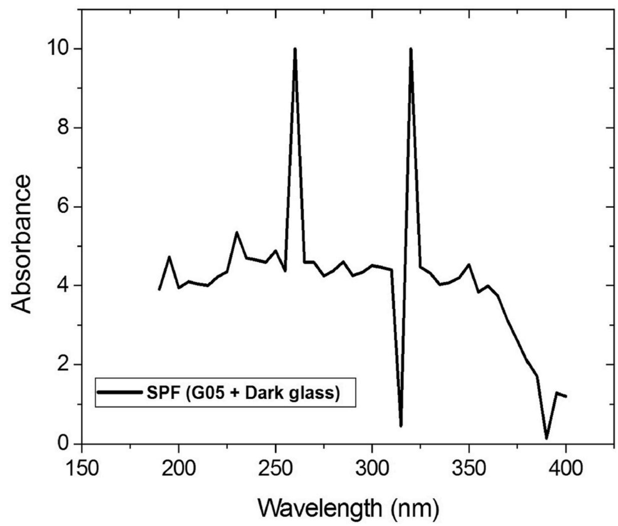

Fig. 2. Absorbance *versus* wavelength in the evaluated region with high Signal-to-noise (SNR) ratio.

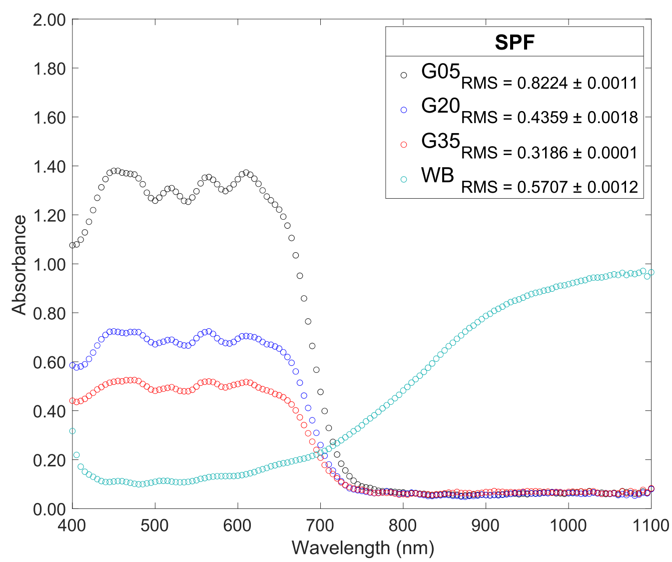

Fig. 3. Absorbance versus wavelength, UV–Vis spectra, in the ROI region for G05, G20, G35 and WB, SPF samples, and its RMS values. The uncertainty of the measurements obtained was lower than 1%. The uncertainty was of type C, which considers the Root sum Squared (RSS) of the uncertainties A (from measurements) and the uncertainties B (from equipment).

measurements are taken in a spectrophotometer equipment, utilized in areas such as Chemistry, Physics and Biology, because it is a non-invasive and non-destructive technique.

Notably, many factors can influence the effectiveness of the UVR blocking capabilities, in the context of the combined use of glass and solar protective films. Some of these factors include the manufacturer origin, the chemical constitution, the thickness, the non-transparent state, the opacity level, the coating and thermal treatments of both glass and solar protective films, and so on. Since the solar films' protective efficacy can vary as a function of the above-cited factors, this work sought to quantify the effects of the glass color and the manufacturer type on the blocking power of UV-radiation using the measured absorbance response curve [22,23].

The UVR protection films combined with glass can be used either in homes, workplaces, or in vehicles; they are mostly made of multiple layers of polyethylene terephthalate [14]. The association of tempered

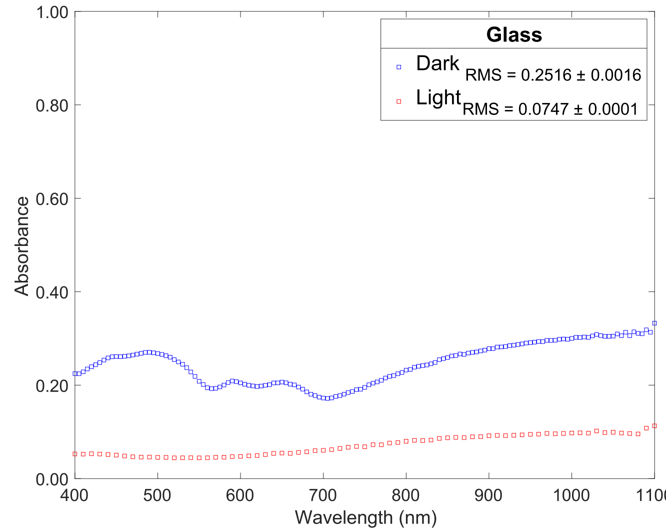

Fig. 4. Comparison between the light and dark glass samples, for absorbance versus wavelength, UV–Vis/NIR spectra, in the ROI region, and their RMS values. The uncertainty of the measurements obtained was lower than 1%. The uncertainty was of type C, which considers the root sum squared (RSS) of the uncertainties A (from measurements) and the uncertainties B (from equipment).

glass and films according to research confirms their effectiveness in blocking rays [15].

3. Materials and methods

For this work, four solar protection film samples were used and named, from here forth, as G05, G20, G35 and WB, the three first manufactured by Window premium® and the fourth one by Window blue®. These acronyms were derived from their respective commercial names. According to the manufacturer, they can provide the blocking of UVR at the levels of 99% for G05, G20, G35, and 100% for WB. Also, the samples G05, G20, G35 present shades of black and with intensities in Visible Light (Vis) of 95%, 80% and 65%, respectively. For the Infrared Radiation (IR) protection , the manufacturer informs that they block 90%, for G05, G20, G35, and 99% for WB. The SFP sample dimensions were 1.0×3.0 cm^2, and the UV–Vis/NIR spectrophotometer (Genesys UV–Vis 10S) readings were taken on an optical step of 1 nm, ranging from 400 nm to 1100 nm.

For the Design of Experiments (DoE) method, it is possible to estimate quantitively the influence of the controllable variables, also known as factors, over the response value, using the Multiple Linear Regression method, as shown in Section 3.1. This work, through DoE, was used to optimize the experimental setup to cover all combinations two-by-two.

3.1. Experimental setup

Seeking to assess the effectiveness of the solar protective films regarding their capability on blocking UVR, Vis and IR rays, two constitutive variables were selected: the glass color, coded as "factor – A″ and the solar protective film of G05, G20, G35, and WB, coded as "factor – B". Besides, to emulate the *ex-situ* condition as a proxy to the operational conditions in which these solar protective films are used, an association was made between the solar protection film and the glasses. Two types of glasses were used in superposition with the solar protective films, the first glass being light, and the second one named dark glass, also called commercial soda-lime glass (Fig. 1); its physical and chemical properties can be found in the literature [24].

Table 1 shows the factors and their respective organization. Factor A corresponds to the solar protective films named as Type 1 and Type 2, and their coded levels −1 and +1. Factor B corresponds to the glasses

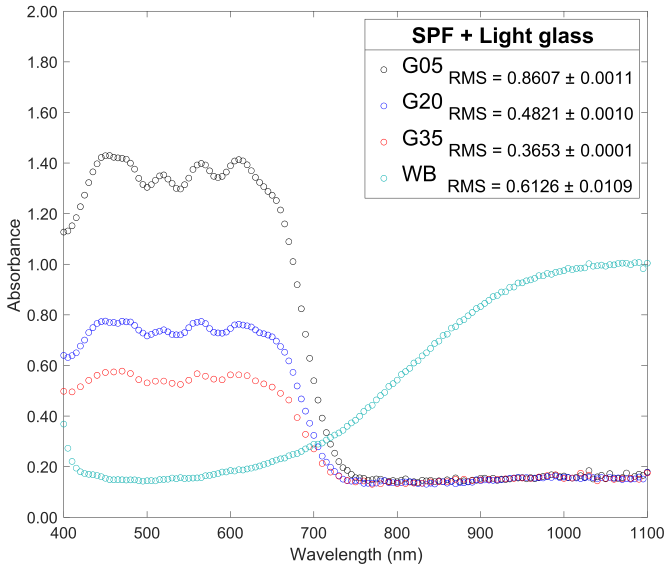

a

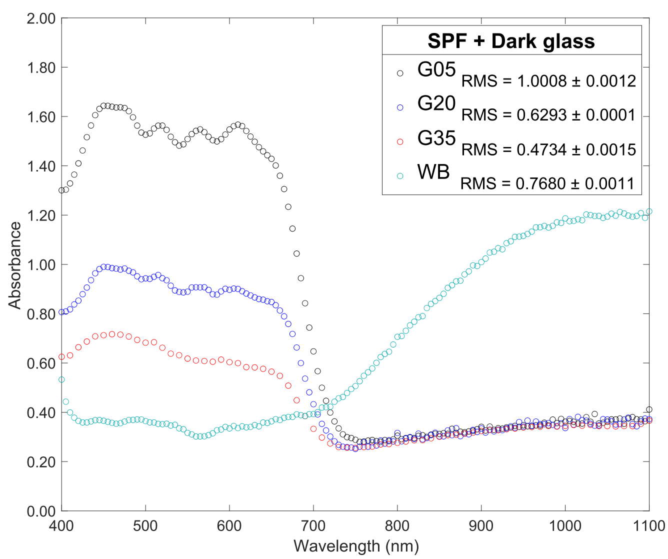

b

Fig. 5. UV–Vis spectra for glass samples associated with solar protective films (G05, G20, G35 and WB): absorbance versus wavelength for: a) Light glass and b) Dark glass. The uncertainty of the measurements obtained was lower than 1%. The uncertainty was of type C, which considers the root sum squared (RSS) of the uncertainties A (from measurements) and the uncertainties B (from equipment).

coded as −1 for dark glass and +1 for light glass.

Table 2 shows all combinations of low and high factor treatments (associated with absorbance measurements) which were designated as experimental runs. This order is standard, and it was used to describe treatment combinations.

Therefore, for the measurements in the spectrophotometer six combinatorial tables were obtained by making the interleaving of films and glasses (Table 3). They were designated by pairs (P) making all interactions between the film and glass samples as follows: P1:G05/G20; P2:G05/G35, P3:G05/WB, P4:G20/G35, P5:G20/WB and P6: G35/WB.

The Root Mean Square (RMS) value for each run was determined using Eq. (2).

$$RMS(i,j) = \sqrt{\frac{1}{(k-n)} \sum_{n}^{k} A_{k,j}^2} \quad (2)$$

where $(k - n)$ is the total number of samples covering the region of interest (ROI) from $n = 400$ nm up to $k = 1100$ nm, for G05, G20, G35 and WB samples; and all with a discrete optical step of 1 nm, $A_{k,j}$ is the corresponding absorbance obtained from the spectrophotometer measurements at the optical length k to the j'th triplicate. The measurement uncertainty, e_i, to the i'th run was taken as the maximum standard deviation between $RMS(i,j)$, and the $\overline{RMS(i,j)}$ (mean value) as shown in Eq. (3):

$$e_i = \max_{1 \le j \le 3} \sqrt{\frac{\sum_{j=1}^{N=3} \left(RMS(i,j) - \overline{RMS(i,j)} \right)}{N-1}} \quad (3)$$

where j indicates the triplicate measurements from absorbance measurements.

The y_i entries in Table 2 (last column) were taken as the mean value of the Root Mean Square (RMS) value derived from the broad range absorbance spectra taken in triplicate. As a result, each y_i was calculated using Eq. (4):

$$y_i = \frac{1}{T} \sum_{j=1}^{T=3} RMS(i,j) \quad (4)$$

where $T = 3$ represents the triplicate measurements, $i = 1$ up to 4, and $j = 1$ up to 3 represent the triplicate measurements in relation to the i'th run.

This same procedure was undertaken for each P'th pair, P1:G05/G20; P2:G05/G35, P3:G05/WB, P4:G20/G35, P5:G20/WB and P6: G35/WB.

3.2. Design of Experiments (DoE)

As mentioned, the DoE method employed was the full 2^k factorial design: the 2^k stands for an experimental setup, which is designed with $k = 2$ controllable factors and each factor has two levels. The main goal of the DoE is to adjust an analytical model, which provides quantitative information about the system response as a function of the combined variation of the input factors.

The 2^k factorial design is adequate to perform analyses when there

Table 4
Factorial design matrix with measurements (run: 1 to 4) and pairs P1: G05/G20; P2: G05/G35, P3: G05/WB, P4: G20/G35, P5: G20/WB and P6: G35/WB. The RMS values from absorbance measurements for each glass and film group can be observed.

Run	X1	X2	X1X2	P1	P2	P3	P4	P5	P6
				G20/G05	G35/G05	WB/G05	G35/G20	WB/G20	G35/WB
1	−1	−1	+1	0.4821 ± 0.0010	0.3653 ± 0.0001	0.6126 ± 0.0109	0.3653 ± 0.0001	0.6126 ± 0.0109	0.3653 ± 0.0001
2	+1	−1	−1	0.8607 ± 0.0011	0.8607 ± 0.0011	0.8607 ± 0.0011	0.4821 ± 0.0010	0.4821 ± 0.0010	0.6126 ± 0.0109
3	−1	+1	−1	0.6293 ± 0.0001	0.4734 ± 0.0015	0.7680 ± 0.0011	0.4734 ± 0.0015	0.7680 ± 0.0011	0.4734 ± 0.0015
4	+1	+1	+1	1.0008 ± 0.0012	1.0008 ± 0.0012	1.0008 ± 0.0012	0.6293 ± 0.0001	0.6293 ± 0.0001	0.7680 ± 0.0011

Table 5

Significance effect values from each group according to the 2^2 factorial design. The values of the non-standardized effects A, B and AB, from Eq. (8). These effects were standardized from Eq. (9). The standard error for non-standardized values was obtained as: $E = \hat{\sigma}\sqrt{\frac{1}{n2^k}}$, where E is the standard error, $\hat{\sigma}$ is the mean square error, n is the number of replicas, e k is the number of levels for the DoE. The standard error for standardized values was obtained as: $E = Z_\alpha\sqrt{\frac{\alpha(1-\alpha)}{n}}$, where E is the standard error, Z_α is the value for the normal distribution for the level of significance α, $(1-\alpha)$ is the confidence level (95%), and n is the number of samples.

	Non-standardized effects					
	P1	P2	P3	P4	P5	P6
A	0.3751 ± 0.0703	0.5114 ± 0.0703	0.2404 ± 0.0703	0.1363 ± 0.0703	−0.1346 ± 0.0703	0.2710 ± 0.0703
B	0.1436 ± 0.0002	0.1241 ± 0.0002	0.1477 ± 0.0002	0.1277 ± 0.0002	0.1513 ± 0.0002	0.1317 ± 0.0002
AB	−0.0036 ± 0.0003	0.0160 ± 0.0003	−0.0077 ± 0.0003	0.0196 ± 0.0003	−0.0041 ± 0.0003	0.0237 ± 0.0003
Standardized effects						
A	1.0654 ± 0.0725	1.1296 ± 0.0723	0.9062 ± 0.0644	0.6429 ± 0.0487	−0.9697 ± 0.0675	1.0392 ± 0.0711
B	−0.1471 ± 0.0113	−0.3573 ± 0.0279	0.1667 ± 0.0130	0.5092 ± 0.0390	1.0277 ± 0.0706	−0.0836 ± 0.0081
AB	−0.9183 ± 0.0650	−0.7723 ± 0.0278	−1.0729 ± 0.0129	−1.1521 ± 0.0390	−0.0580 ± 0.0706	−0.9556 ± 0.0081

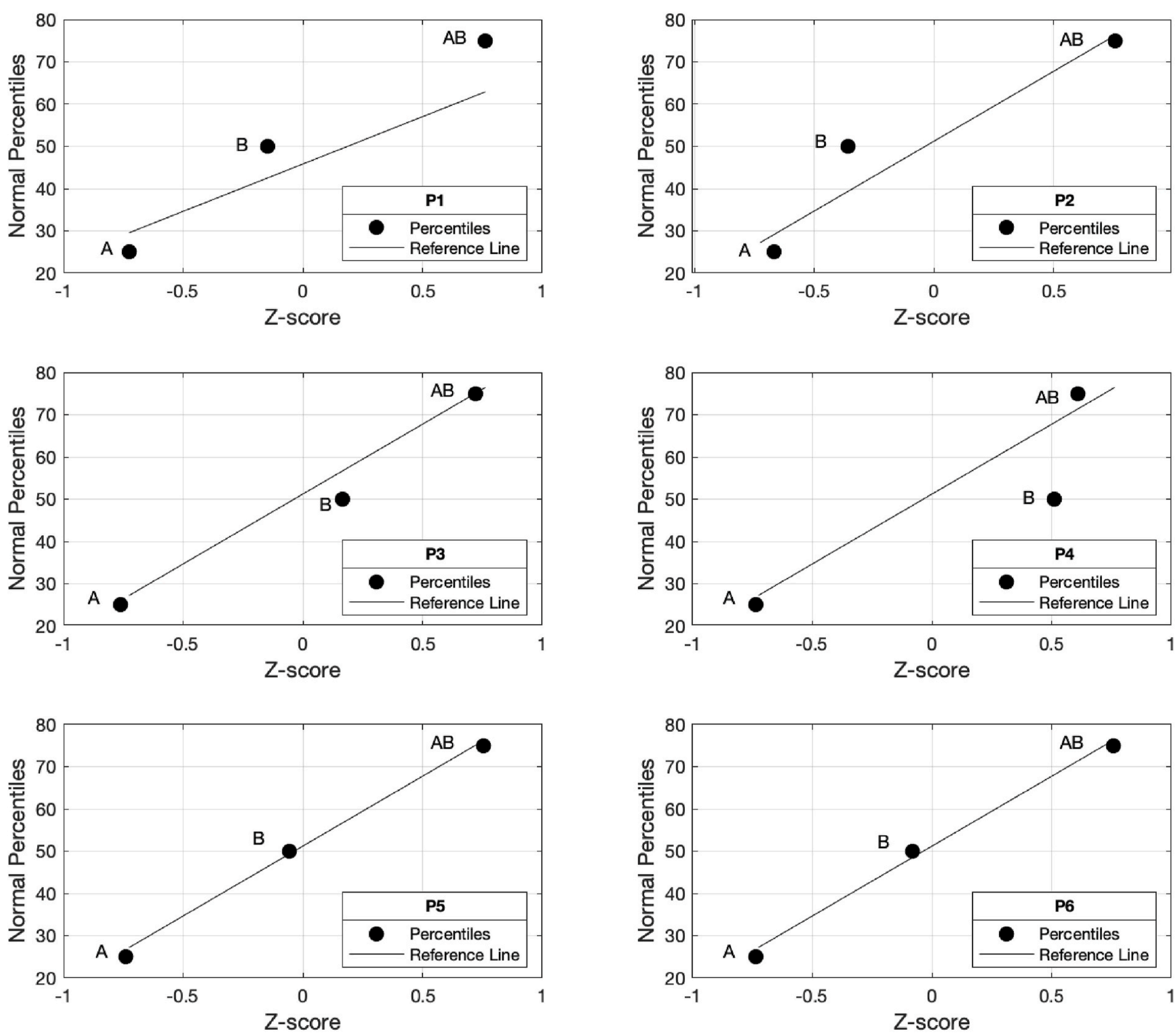

Fig. 6. Normal percentiles versus Z-score from the groups P1: G05/G20; P2: G05/G35, P3: G05/WB, P4: G20/G35, P5: G20/WB and P6: G35/WB. The results for effects A, B and AB also are presented.

are several experimental interactions between the relevant controllable variables, or factors$X$, that can produce a variation on the system response, y. Montgomery and Runger [11] state that the factorial design can be expressed in terms of a Multiple Linear Regression (MLR) model. Since the number of measurements, $n = 4$, is greater than the number of regressive variables, a model representing the absorbance originated from the interaction between glasses and protective films can be set properly using Eq. (5):

$$y_i = \beta_0 + \beta_1 x_{i1} + \beta_2 x_{i2} + \cdots + \beta_k x_{ik} + \varepsilon_i \tag{5}$$

where y_i represents the model's output according to "n" taken measurements with i = 1, 2, …, n, x_{i1} represents the coded factor A, x_{i2}

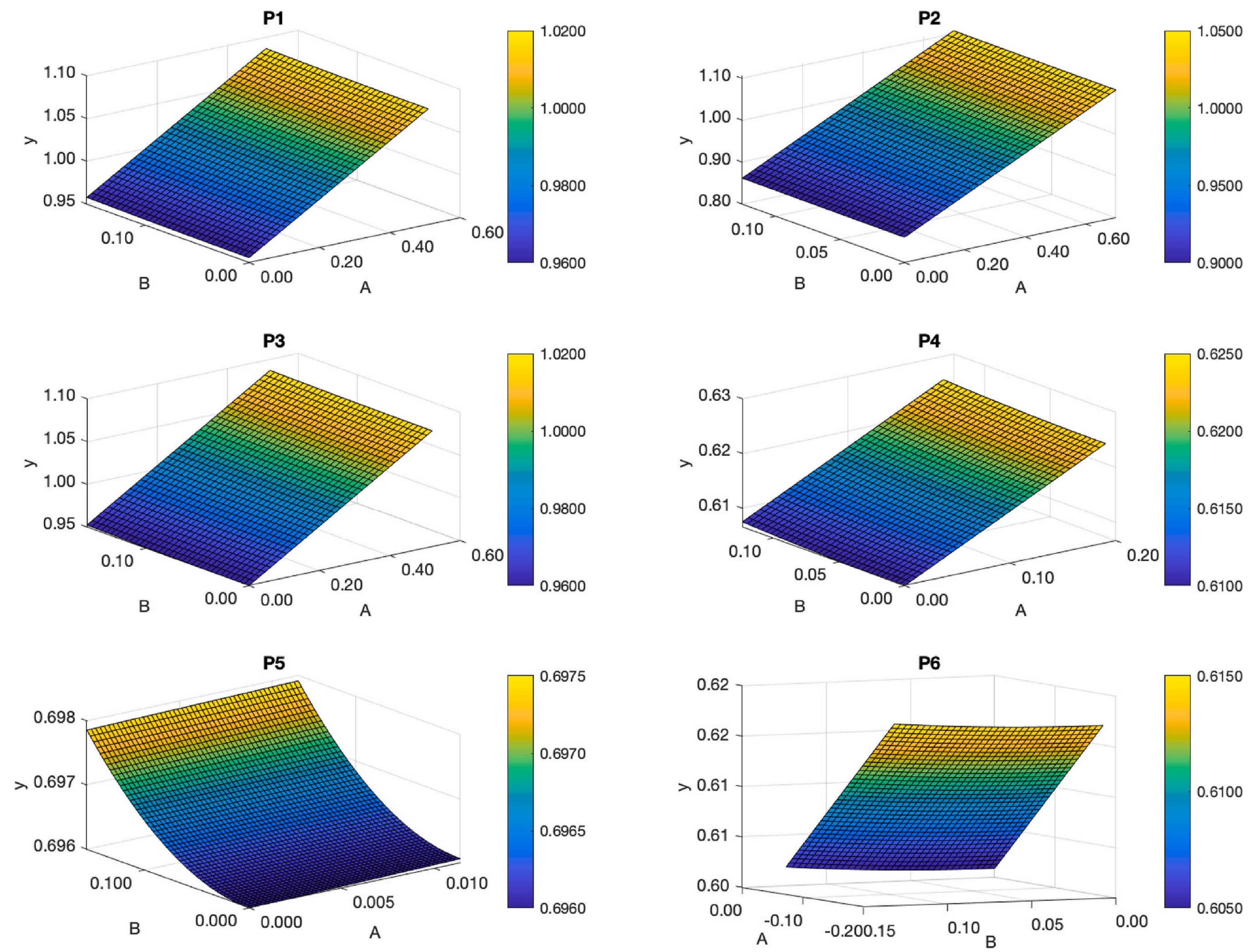

Fig. 7. Response surface of y (MLR output), showing the sensitivity of this function in relation to effects A and B.

represents the factor B, and x_{i3} represents the AB interaction. Equation (5) can be expressed in a matrix form, shown by Eqs. (6) and (7), respectively:

$$y = X\beta + \varepsilon \tag{6}$$

where in Eq. (6) the terms correspond to:

$$y = \begin{bmatrix} y_1 \\ \vdots \\ y_n \end{bmatrix}; \quad X = \begin{bmatrix} 1 & \cdots & x_{1k} \\ \vdots & \cdots & \vdots \\ 1 & \cdots & x_{nk} \end{bmatrix}; \qquad \beta = \begin{bmatrix} \beta_0 \\ \vdots \\ \beta_k \end{bmatrix} \text{ and } \varepsilon = \begin{bmatrix} \varepsilon_1 \\ \vdots \\ \varepsilon_n \end{bmatrix} \tag{7}$$

Based on the regression coefficients β_1, β_2 and β_3 and from the Montgomery and Runger definition [11], ε is error, the effects of A, B, AB were calculated as the double of the regression coefficients β_1, β_2 and β_3 respectively. The $\beta_0$is the global mean; then, according to Montgomery and Runger [11], applying the MLR method, it is possible to find the regression coefficients β through the estimator $\widehat{\beta}$, which can be written as Eq. (8):

$$\widehat{\beta} = (X'X)^{-1}X'y \tag{8}$$

where X' and $(X'X)^{-1}$ are the transposed and inverse matrices, respectively. As seen, from the values of the regression coefficients, it is possible to determine an analytical model for the system under study.

Montgomery and Runger [11] suggested that the regressors must be standardized using the z-score, see Eq. (9). The new values in the mapped z-score space allow a fair comparison of the same effects, A, B and AB within different experimental setups. Moreover, this procedure seeks to highlight the most significant effects when their values are plotted on a cumulative normal percentile graph.

$$z_i = \left(\beta_i - \mu\left(\widehat{\beta}\right)\right) / \sigma\left(\widehat{\beta}\right) \tag{9}$$

where μ is the mean value operator, σ is the standard deviation operator, z_i is the standardized effect, with $i = 1$, 2 and 3 corresponding to the effects A, B, AB respectively.

3.3. Inferential statistical analysis

The one-way analysis of the variance test, or one-way ANOVA test, was used to verify if the solar protection film types: G05, G20, G35, and WB, coded previously as the Effect – A was statistically significant, with relation to the mean net absorbance readings, given by Eq. (10):

$$\overline{A}_k = \frac{1}{T}\sum_{j=1}^{T=3} A_{k,j} \tag{10}$$

where $\overline{A}_k$ is a vector corresponding to the mean absorbance readings from the triplicates, along with an ROI varying from $k = 400$ nm up to 1100 nm, for G05, G20, G35, and WB samples, and simultaneously

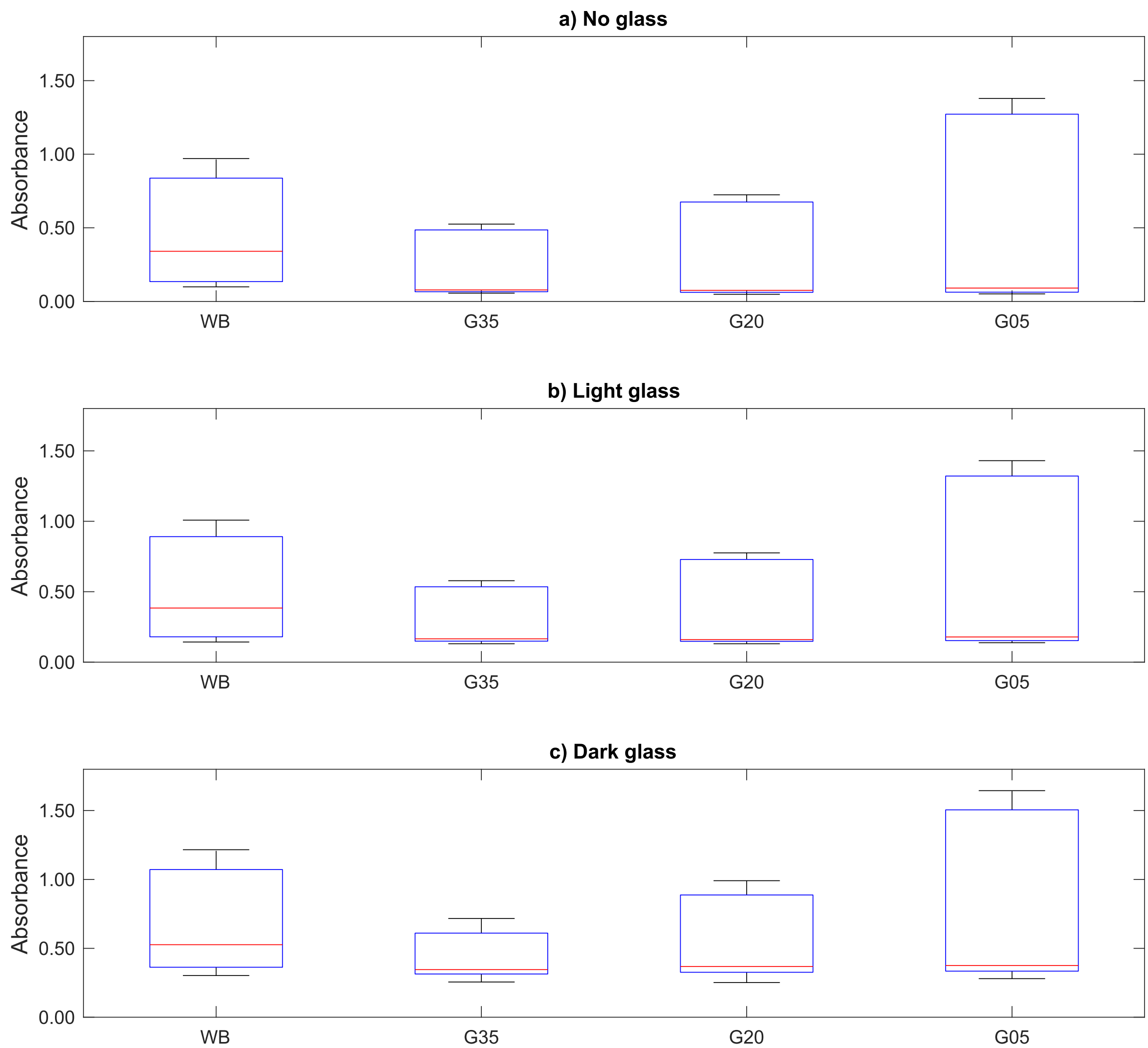

Fig. 8. Boxplot of the absorbance versus WB, G35, G20 and G05 solar protective film samples and glasses. Results for the medians were placed in ascending order for the pairs G35, G20 and G05, and for WB the increase can be observed through the change in each graph such as: a) no glass, b) light glass and c) dark glass.

encompassing all the j'th samples for each triplicate.

The mean absorbance of each solar protective film was identified by $\mu_g$where $\mu_g = \mu((\overline{A}_k)^g)$, with μ representing the mean operator and g representing a sample from the set $g = \{G05, G20, G35, WB\}$The employed ANOVA statistical test of significance is given as follows, Eq. (11):

$$\begin{cases} H_0 : \mu_1 = \mu_2 \\ H_1 : \mu_1 \neq \mu_2 \end{cases} \tag{11}$$

This test can be understood as: given a null hypothesis, H_0, that is true, if and only if, the mean values μ_1 and μ_2 derived from normal distributions are equal under a certain level of uncertainty, expressed through the p-value. The p-value adopted in this work was set as 0.05. A p-value < 0.05 implies the rejection of the null hypothesis, leading to the adoption of H_1, informing that the sample data are not derived from the same normal distribution, thus making the leading factor to be statistically significant.

Since the one-way ANOVA test only reveals if there is a significant difference between the mean values of the factors, the two-way Bonferroni Test was used to identify within the two factors, which are those that show the greatest significance difference in terms of the mean value.

3.4. Validation of DoE and MLR methods

When applying the DoE and MLR methods, the responses will be the predicted values and real values from the absorbances values from the UV–Vis/NIR equipment. To validate the methods the statistical error metrics were used, such as the Root Mean Square Percentage Error (RMSPE), Eq. (12), and the Mean Absolute Percentage Error (MAPE), Eq. (13), as follows:

$$RMSPE = \sqrt{\frac{1}{n}\sum_{i=1}^{n}\left(\frac{y_i - \hat{y}_i}{y_i}\right)^2} \text{x}100\% \tag{12}$$

$$MAPE = \sqrt{\frac{1}{n}\sum_{i=1}^{n}\left|\frac{y_i - \hat{y}_i}{y_i}\right|} \text{x}100\% \tag{13}$$

where y_i are the real values, $\hat{y}_i$ are the predicted values, and n is the number of data used in the prediction. The RMSPE and MAPE error metrics were used as a benchmarking criterion for the goodness of the fitting characteristics for the predicted values such as: $<$ 10% highly accurate, 10%–20% good, 20%–50% reasonable, $>$ 50% inaccurate [24]. These statistical error metrics are used to calculate the forecast power, to estimate the performance and reliability of the model

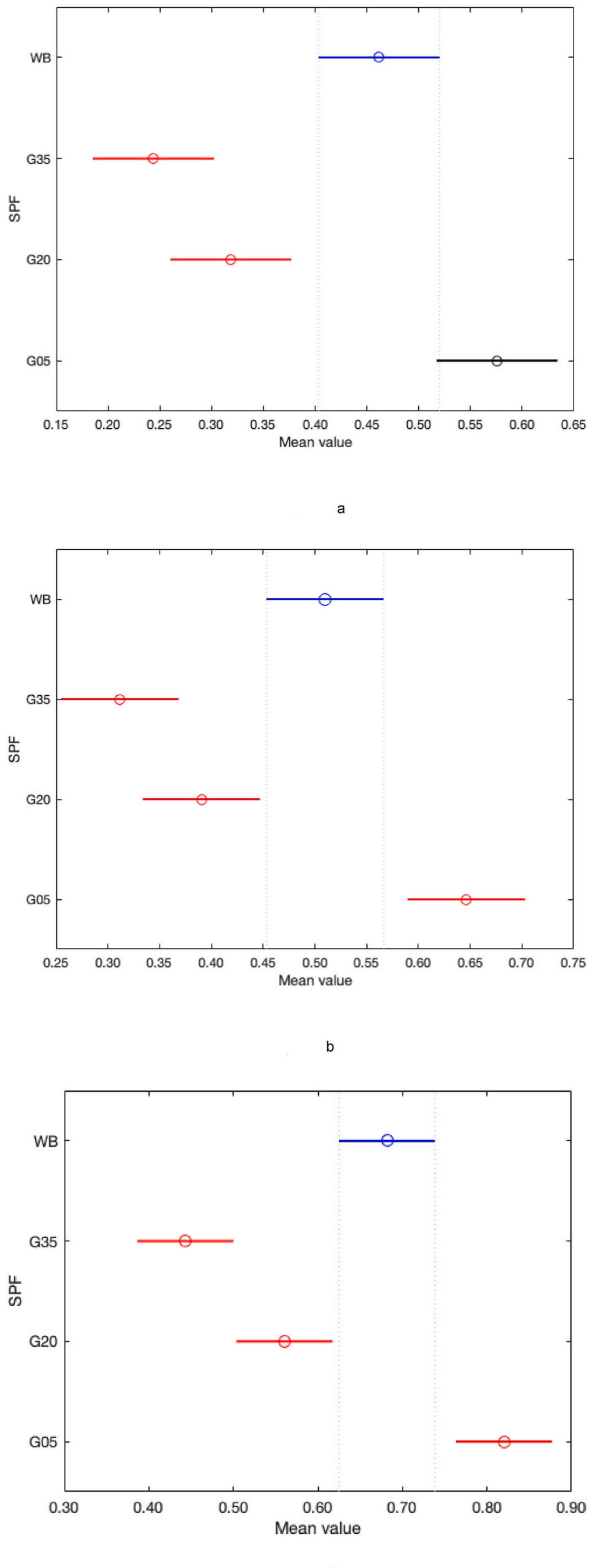

Fig. 9. Bonferroni Test, mean values of each group WB, G35, G20 and G05. The horizontal line for each element of the group is the mean value, if these horizontal lines have their disjoint intervals then they are significantly different, otherwise they are not significantly different. The possibilities of samples with glasses are: a) no glass, b) light glass and c) dark glass are shown.

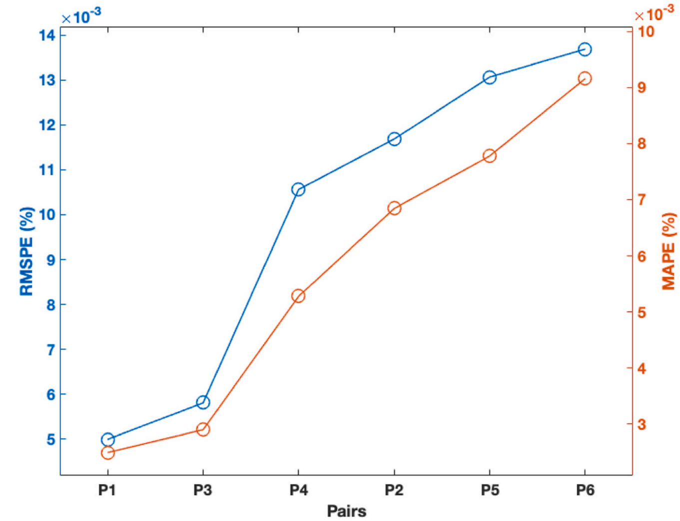

Fig. 10. Root Mean Square Percentage Error (RMSPE), and Mean Absolute Percentage Error (MAPE) *versus* pairs (P1, P3, P4, P2, P5 and P6) in increasing order of their values compared to statistical error methods.

employed to make the predictions.

4. Results and discussion

4.1. Absorbance analysis

Measurements in the region comprised between 190 nm and 380 nm were performed for the SPF + dark and light glass samples. For these associations, this region presents higher absorbance values for the detection limit of the UV–Vis/NIR equipment, and these values also contain the influence of noise/signal from the analyzed region; these effects would be inappropriate to the methods applied in the results of scientific research; therefore, this region (190 nm–380 nm) was removed from results. Fig. 2 presents absorbance *versus* wavelength in the region with noise; similar results were obtained with the other samples of glass and SPF.

Fig. 3 shows the comparison of absorbance spectra from solar protective films without any glass layering. As observed, there is a notable similarity in terms of curve shapes to the films G05, G20 and G35. For the film WB, in the visible region, low absorbance values are noted, that is, an almost transparent film, and in the posterior region, 800 nm–1100 nm, the values increase because this film blocks the infrared rays in 100%. The absorbance values in the visible region are decreasing in relation to the films G05, G20 and G35, as they let the incident light pass through 95%, 80% and 65% respectively. In the ultraviolet region, these rays are practically blocked and in the infrared the absorbance values tend to be zero. On the other hand, the absorbance magnitude expressed in terms of the RMS value varied significantly as: 0.8224 ± 0.0011, 0.4359 ± 0.0018, 0.3186 ± 0.0001, 0.5707 ± 0.0012 for G05, G20, G35, and WB SPF respectively. This result shows descriptively that the manufacturer's origin provided a substantial influence on Vis and NIR region. Typical measurements of SPF and glasses have been reported on various types of materials. The results presented in the literature [25,26] are adequate and demonstrate that they can be obtained by measuring the Vis and NIR regions, as shown in this work (Fig. 3).

4.2. Combined analysis

Differently from Section 4.1, the results are now presented considering the layering of glass types, that could be light or dark, with the solar protective film types grouped as G05, G20, G35, and WB. Fig. 4 shows only the glass without the layering with solar protective films. For light and dark glasses, the absorbance, RMS values at all wavelengths are less than 0.12 and 0.34; 0.0747 ± 0.0001, 0.2516 ± 0.0016, respectively. For the Vis region, the contribution of the absorbance values of dark glass is significant, and in the NIR region, dark glass shows a larger contribution than light glass. In the case of the absorbance values for the light glasses, there is a contribution in the region between 0.0410 and 0.0810 of absorbance; in the Vis and NIR regions, the values are then between 0.0820 and 0.1130, respectively. These results show the contribution of glasses to the evaluation of the association of glasses and films. New materials have been evaluated to be used as solar protection film [27,28], and the results demonstrate the interest in the Vis and NIR spectral regions as adopted in this work.

Fig. 5a and b shows the spectra measurements derived from all combinations of glasses and solar protective films taken at a specific ROI (ranging from 400 nm to 1100 nm). These results indicate that both light and dark glasses in association with solar protective films produced in the ROI have different RMS values. The samples G05, G20 and G35 are more efficient in the Vis region, showing discrete values according to their tones. The WB sample is more efficient in the NIR region than the Vis region. As can be seen, at a global level, using the RMS values from the light and dark glass groups as a metric, the dark glass in combination with the solar protective films, Fig. 5b, showed larger absorbance values than the light glasses, Fig. 5a. The relative percentages for associations with SPF and dark glasses compared to SPF and light glasses were 14%, 23%, 23% and 20% for G05, G20, G35 and WB, respectively. These results can be misleading, ever since users may consider that dark materials provide better photoabsorption properties. The definition of the ROI, the opacity of the samples and the evaluations of the absorbances, are in agreement with previous works found in the literature [29].

Table 4 shows the RMS values of absorbance measurements for each SPF and glass group: P1, P2, P3, P4, P5, and P6. The results provided the y responses to be applied in Eq. (8), which is important in determining regression coefficients. The maximum uncertainty obtained was lower than 1.09% for all combinations. Subsequently, the factors A and B varied discretely from the levels −1 to +1, which means that the system response was taken respectively from the lowest to the highest state. The total information for each P pair can be expressed by the sum of all run possibilities (each column of Table 4), for the pairs P1, P2, P3, P4, P5 and P6 the sums are: 2.9729, 2.7002, 3.2421, 1.9501, 2.4920, and 2.2193, respectively. In decreasing order, the values of the P pairs are: P3 > P1 > P2 > P5 > P6 > P4. These results indicate the strong contribution of the WB/G05 pair to both absorption in the Vis and NIR regions, followed by the pairs G20/G05, G35/G05, G20/WB, G35/WB and G35/G20, respectively.

Table 5 shows results for the regression values obtained using Eq. (8); they were standardized via Eq. (9), and plotted on a normal percentile versus z-score in Fig. 5, which shows the normal percentile versus z-score for the groups (P1, P2, P3, P4, P5 and P6).

Based on Fig. 6, within all of those six groups, it was possible to show that the glass color, encoded to the factor (B), varying from −1 to +1, or from a light glass to a dark glass, the absorbance response was irrespective to it. Contrarily, the most significant effect was the automotive solar protector film (A), as can be seen in Fig. 6, where factor (A) is far away from the origin of the normal distribution plot. The statistical analysis of the results pointed out an agreement between Section 4.1 and Section 4.2 results, where the factor A, in magnitude, was superior to the glass type, the factor B. Therefore, one may argue that using the right solar protective film can be more advantageous than designing a doped glass. Under a qualitative analysis, all of the group responses agreed that the interaction effect (AB) has had a positive impact on the absorbance; in other words, as AB varied from −1 to +1 the absorbance increased, then showing that the glass association with the solar protective films increased the overall absorbance.

Fig. 7 shows the results of y (from Eq. (5)) *versus* effects A and B. This evolution of the effects from zero up to their maximum values, provides information about which of these factors obtained has the greatest influence of the SPF + glasses system. The pairs of groups P1, P2, P3 and P4 have an increase in effect A increasing in relation to effect B, which practically remains constant. The pairs of groups P5 and P6 show an increase in effect B increasing in relation to effect A, which practically remains constant. It is worth mentioning that these results are from Eq. (5). This equation contains elements of interaction AB, A and B effects of total beta media that can also influence the pair combination.

4.3. ANOVA and Bonferroni Test analyses

Fig. 8a, b and c show the boxplot of the absorbance for each solar protective film in association with no glass, with light glass and dark glass, respectively. These results provide information about the mean values for the SPF and glass associations; the mean values are well distributed in an increasing order for all combinations coming from G05, G20 and G35; for the WB results it is also possible to observe the increase in the results for no glass, with light glass and with dark glass. On each box, the central mark indicates the median, and the bottom and top edges of the box indicate the 25th and 75th percentiles, respectively. Another important fact is the absence of outliers for all combinations.

Employing the one-way ANOVA test, the results for the factor corresponding to the manufacturing origin was statistically significant with p-value < 0.05. From these results, it can be inferred that hypothesis H_1 is the correct one, thus implying the rejection of the null hypothesis.

Solar protective film samples *versus* mean values, using the Bonferroni Test (multiple comparisons) for no glass, light glass and dark glass are presented in Fig. 8a, b and c, respectively. The WB sample in this figure was considered the control term, and its color is blue, and the other SPFs present red color, the pair group means are significantly different. In Fig. 9a, the pairs WB/G35 and WB/G20 are significantly different, but WB/G05 is not different; this result is shown in black. In Fig. 9b and c, all combinations, WB/G35, WB/G35 and WB/G05 are significantly different. Hence, as expected, the combined analysis can be proceeded satisfactorily due to the absence of collinearity among the y responses.

4.4. Validation of DoE and MLR methods

RMSE and MAPE *versus* pairs of association with all SPF samples are presented in Fig. 10. The accuracy for the prediction of the DoE method together with the MLR method in SPF + glass measurements was excellent. It agrees with the low values obtained for the RMSPE and MAPE errors, which present minimum and maximum values of 0.0049% up to 0.0137% and of 0.0024% up to 0.0091%, respectively. The groups as shown in the figure are in ascending order for the RMSPE and MAPE values, and the groups with the best accuracy are as follows: P1 > P3 > P4 > P2 > P5 > P6. The use of DoE and consequently its validation present enough evaluation for the accuracy of the method used, as well as the evaluation and usefulness of other statistical methods that can be found in the literature [30]. They agree with the results of this work.

5. Conclusions

From the results it can be stated that: i) the absorbance values for SPF and light and dark glass samples can be determined via UV–Vis/NIR measurements; ii) the contribution to the absorbance values, in the visible and in the infrared regions, for dark glass is more significant than for light glass; iii) G05, G20 and G35 are more efficient in the Vis region, and the WB sample is more efficient in the NIR region than in the Vis region, in comparison with G05, G20, and G35 samples; iv) For the RMS results in all regions, the descending order was given by P3 > P1 > P2 > P5 > P6 > P4, indicating a greater contribution from the WB/G05 pair presenting absorption in the Vis and NIR regions; v) the factor A showed higher absorbance values compared to the glass type, the factor B; vi) the results also showed the strong influence of the AB interaction in the application of methods within the mean values of beta coefficients; vii) through the results of the one-way ANOVA test, the samples showed p-value < 0.05, indicating the statistical difference of the data from the absorbances; however, it was still necessary to find out which pair would be indicated with the greatest or least significant difference; this was resolved with the use of the Bonferroni Test (multiple comparison) which indicated according to the determined standard which mean values would be different; in the majority, the groups showed good results and indicated as conclusion the absence of collinearity among the y responses; viii) the RMSPE and MAPE methods presented statistically excellent accuracy values, with the highest value of 0.0137%, that is, the error between the measured and the predicted values was less than 0.014%, concluding that these statistical error methods can be applied for the determination of the accuracy in the DoE and MLR methods in measurements from glass and SPF absorbances. The results obtained in this work can be useful in the association of SPF + glasses in the medical area, in industries, agriculture, automobile, and even in sustainable houses, as well as in the evaluation of new materials. They need a robust evaluation such as the DoE, to be used in the investigation of sun protection of people. In conclusion, the Design of Experiments (DoE) and Multiple Linear Regression (MLR) methods are suitable to be used in the investigation of the materials evaluated in this work.

Credit author statement

Eriberto Oliveira do Nascimento: Conceptualization, Validation Methodology, Software, Formal analysis, Data curation, Writing – review & editing. Matheus José Pires Becatti: Data Curation. Linda V.E. Caldas: Methodology, Supervision, Writing – review & editing, Funding acquisition. Lucas Nonato de Oliveira: Conceptualization, Methodology, Validation, Formal analysis, Resources, Data curation, Investigation, Resources, Writing – original draft, Writing – review & editing, Visualization, Funding acquisition.

Declaration of competing interest

The authors declare that they have no known competing financial interests or personal relationships that could have appeared to influence the work reported in this paper.

Acknowledgments

The authors thank the Brazilian funding agencies CNPq (Grants 104486/2019–8, 164981/2020–9 and 301335/2016–8) and FAPESP (Project 2018/05982–0) for partial financial support.

References

[1] B.L. Diffey, Ultraviolet radiation physics and the skin, Phys. Med. Biol. 25 (1980) 405.
[2] J. Cadet, E. Sage, T. Douki, Ultraviolet radiation-mediated damage to cellular DNA, Mutat. Res. Fund Mol. Mech. Mutagen 571 (2005) 3–17.
[3] A.E. Stapleton, V. Walbot, Flavonoids can protect maize DNA from the induction of ultraviolet radiation damage, Plant Physiology 105 (1994) 881–889.
[4] C. Backes, A. Religi, L. Moccozet, F. Behar-Cohen, L. Vuilleumier, J.-L. Bulliard, D. Vernez, Sun exposure to the eyes: predicted UV protection effectiveness of various sunglasses, J. Expo. Sci. Environ. Epidemiol. 29 (2019) 753–764.
[5] F. Almutawa, R. Vandal, S.Q. Wang, H.W. Lim, Current status of photoprotection by window glass, automobile glass, window films, and sunglasses, Photodermatology, Photoimmunology & Photomedicine 29 (2013) 65–72.
[6] S. Heydarian, M. Mahjoob, A. Gholami, S. Veysi, M. Mohammadi, Prevalence of color vision deficiency among arc welders, Journal of Optometry 10 (2017) 130–134.
[7] H. Nakashima, J. Takahashi, N. Fujii, T. Okuno, Blue-light hazard from gas metal arc welding of aluminum alloys, Annals of Work Exposures and Health 61 (2017) 965–974.
[8] M.G. Kimlin, A. v Parisi, Ultraviolet radiation penetrating vehicle glass: a field based comparative study, Phys. Med. Biol. 44 (1999) 917.
[9] D.S. Rigel, Cutaneous ultraviolet exposure and its relationship to the development of skin cancer, J. Am. Acad. Dermatol. 58 (2008) S129. –S132.
[10] K.J. van der Pal, M. Maric, W. van Bronswijk, S.W. Lewis, Ultraviolet-visible spectroscopic characterisation of automotive window tints for forensic purposes, Analytical Methods 7 (2015) 5391–5395.
[11] D.C. Montgomery, G.C. Runger, Applied Statistics and Probability for Engineers, (With CD), John Wiley & Sons, 2007.
[12] D.C. Montgomery, Design and Analysis of Experiments, John wiley & sons, 2017.
[13] M.J. Adams, Chemometrics in Analytical Spectroscopy, Royal Society of Chemistry, 2007.
[14] M. Gogoi, A. Gogoi, UV ray protection property and natural dye, Internat. J. Appl. Home Sci. 3 (2016) 159–164.
[15] C. Tuchinda, S. Srivannaboon, H.W. Lim, Photoprotection by window glass, automobile glass, and sunglasses, J. Am. Acad. Dermatol. 54 (2006) 845–854.
[16] A. Dementjev, V. Gulbinas, L. Valkunas, H. Raaben, Nonlinear absorption of PbS nanocrystals in silicate glass, Phys. Status Solidi 241 (2004) 945–951.
[17] V. de Giuli, R. Zecchin, L. Corain, L. Salmaso, Measured and perceived environmental comfort: field monitoring in an Italian school, Appl. Ergon. 45 (2014) 1035–1047.
[18] N. Kakitsuba, Comfortable indoor lighting conditions for LEDlights evaluated from psychological and physiological responses, Appl. Ergon. 82 (2020) 102941.
[19] W.J.M. van Bommel, Non-visual biological effect of lighting and the practical meaning for lighting for work, Appl. Ergon. 37 (2006) 461–466.
[20] M. Engholm, L. Norin, D. Åberg, Strong UV absorption and visible luminescence in ytterbium-doped aluminosilicate glass under UV excitation, Opt Lett. 32 (2007) 3352–3354.
[21] W. Mäntele, E. Deniz, UV–VIS Absorption Spectroscopy, Lambert-Beer reloaded, 2017.
[22] J. Li, X. Zhang, H. Zhao, J. Zhang, H. Geng, H. Wu, Y. Gu, C. Cheng, X. Qi, Novel transparent Er3+ doped perovskite glasses fabricated by containerless solidification, J. Lumin. 223 (2020) 116892.
[23] N.M. Trindade, M.G. Magalhães, M.C. dos Santos Nunes, E.M. Yoshimura, L. G. Jacobsohn, Thermoluminescence of UV-irradiated α-Al2O3: C, Mg, J. Lumin. (2020) 117195.
[24] L. Zhang, Y. Zheng, K. Wang, X. Zhang, Y. Zheng, An optimized Nash nonlinear grey Bernoulli model based on particle swarm optimization and its application in prediction for the incidence of Hepatitis B in Xinjiang, China, Comput. Biol. Med. 49 (2014) 67–73, https://doi.org/10.1016/j.compbiomed.2014.02.008.
[25] X. Li, W. Liu, W. Zhao, S. Huang, W. Huang, J. Shi, A. Han, J. Li, H. Chen, L. Zhang, F. Meng, Z. Liu, Highly crystallized tungsten doped indium oxide film stabilizes silicon heterojunction solar cells in sodium environment, Sol. Energy Mater. Sol. Cell. 233 (2021) 111387, https://doi.org/10.1016/J.SOLMAT.2021.111387.
[26] H. Salehi, A. Eshaghi, M. Rezazadeh, H. Zabolian, Antireflective and anti-dust modified silica based thin film on solar cell cover glass, J. Alloys Compd. 892 (2022) 162228, https://doi.org/10.1016/J.JALLCOM.2021.162228.
[27] K. Gao, H. Shen, Q. Wei, Y. Liu, I. Ahmad, Reduced thermal effect of AZO/Cu/AZO infrared filter film for solar cell, Opt. Mater. 110 (2020) 110534, https://doi.org/10.1016/J.OPTMAT.2020.110534.
[28] W.C. Du, J. Xie, L. Xia, Y.J. Liu, H.W. Yang, Y. Zhang, Study of new solar film based on near-infrared shielding, J. Photochem. Photobiol. Chem. 418 (2021) 113410, https://doi.org/10.1016/J.JPHOTOCHEM.2021.113410.
[29] P.K. Nair, A.L. Espinosa-Santana, L. Guerrero-Martínez, A. López-Ortiz, M.T. S. Nair, Prospects toward UV-blue filtered solar drying of agricultural farm produce using chemically deposited copper chalcogenide thin films on cellular polycarbonate, Sol. Energy 203 (2020) 123–135, https://doi.org/10.1016/J.SOLENER.2020.04.012.
[30] L.A. Bacci, L.G. Mello, T. Incerti, A. Paulo de Paiva, P.P. Balestrassi, Optimization of combined time series methods to forecast the demand for coffee in Brazil: a new approach using Normal Boundary Intersection coupled with mixture designs of experiments and rotated factor scores, Int. J. Prod. Econ. 212 (2019) 186–211, https://doi.org/10.1016/J.IJPE.2019.03.001.